4-2015

Investigations into Uncharacterized Radical S-adenosylmethionine Enzymes

Melissa Quintanilla
College of Saint Benedict/Saint John's University

Investigations into Uncharacterized Radical S-adenosylmethionine Enzymes

AN HONORS THESIS

College of St. Benedict/St. John's University

In Partial Fulfillment
of the Requirements for All College Honors
and Distinction
in the Department of Chemistry
by

Melissa Quintanilla

April 2015

ABSTRACT

Radical *S*-adenosylmethionine (SAM) enzymes are a superfamily of enzymes that require the cofactor SAM for catalysis. These enzymes have diverse functions across all 3 domains of life, and are known to play roles in many biological pathways, including vitamin biosynthesis, synthesis of complex metal clusters, posttranslational RNA modification, DNA repair, and development of antibiotic resistance, among others. Radical SAM enzymes are characterized by the CX_3CX_2C motif, which is conserved throughout most members of the family. A number of genes have been identified which contain the CX_3CX_2C motif and other amino acid sequences characteristic to radical SAM enzymes, however the majority of these suspected members of the radical SAM superfamily remain poorly understood. To date, only 14 enzymes out of the suspected 50,000 have been fully characterized, including a crystal structure. In order to gain a more complete understanding of the superfamily and their biological significance, it is therefore essential that more of these suspected enzymes are characterized.

For this project, two of these uncharacterized genes were chosen from the structure-function linkage database (SFLD) for further study. The first, referred to as yfgB, showed sequence similarity to the class A radical SAM methyltransferases, and was picked based on the presence of a homolog in the BL21(DE3) *E. Coli* genomic DNA available to the laboratory. This homolog was successfully amplified via polymerase chain reaction (PCR) and sequentially digested with restriction enzymes Blp1 and BamH1, and is now ready to be ligated into the bacterial expression vector pet14b. The second gene, referred to as RS11, codes for an uncharacterized radical SAM enzyme in subgroup 11 (from *Thermotoga neapolitana* DSM 4359, NCBI taxonomy ID: 309803). This subgroup is pyridoxal phosphate (PLP)-dependent, and members show sequence homology to aminomutases. A pEX-N-His bacterial expression vector was purchased with the RS11 gene inserted from Blue Heron Gene Company and transformed into BL21(DE3) *E. Coli*. Attempts to express the RS11 gene and purify the corresponding protein have been unsuccessful thus far.

1. BACKGROUND

Radical *S*-adenosylmethionine (SAM) enzymes are a superfamily of enzymes that require the cofactor SAM for catalysis.[1] These enzymes have diverse functions across all 3 domains of life, and are known to play roles in many biological pathways, including vitamin biosynthesis,[2,3] synthesis of complex metal clusters,[4] posttranslational RNA modification,[5,6] development of antibiotic resistance,[7,8] and DNA repair,[9] among others.

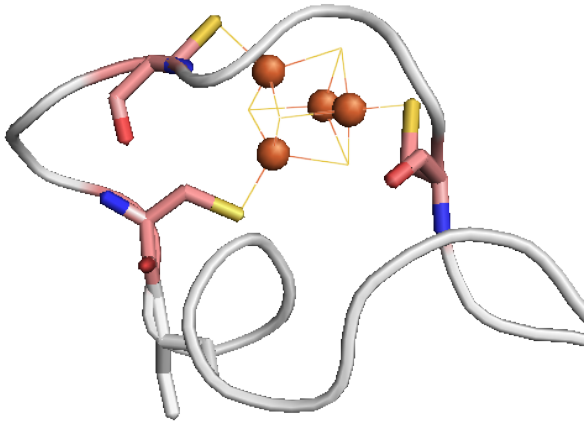

Figure 1.1. Three irons of [4Fe-4S] cluster are coordinated by characteristic CX_3CX_2 motif of radical SAM enzymes (PDB ID 3RF9).

There is limited sequence homology between the enzymes of this superfamily,[10] however many radical SAM enzymes are characterized by a CX_3CX_2C motif,[10,11] The 3 cysteine residues of this motif coordinate with three irons of a [4Fe-4S] cluster utilized by all radical SAM enzymes for catalysis (*Figure 1.1*). The cofactor SAM is also required for catalysis, coordinating with the fourth unique iron of the [4Fe-4S] cluster in a bidentate fashion (*Figure 1.2*).[10,11,12] In many radical SAM enzyme-catalyzed reactions SAM is used as a cosubstrate and is consumed during the reaction, however some radical SAM enzymes use the molecule catalytically and are able to regenerate SAM.

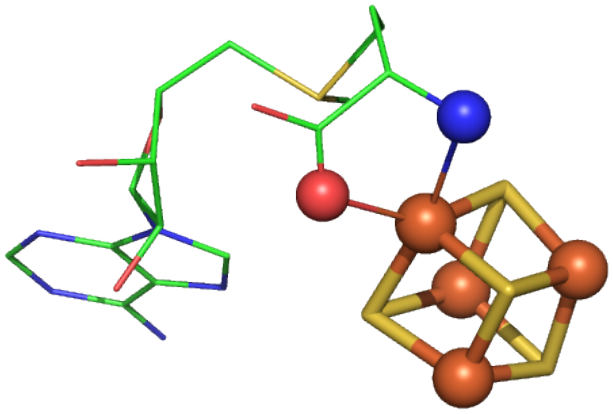

Figure 1.2. Bidentate coordination of the fourth unique iron of [4Fe-4S] cluster by cofactor SAM in radical SAM enzymes.

Knowledge about the structure of radical SAM enzymes is somewhat limited, as only 14 radical SAM enzyme structures have been successfully characterized using X-ray crystallography thus far. However, all characterized structures do share one unifying feature – the triose phosphate isomerase (TIM) barrel (*Figure 1.3)*. The size of the TIM barrel can vary based on the individual enzyme, however a full TIM barrel

consists of eight sets of alternating α helices and β strands, with the β strands contained on the inside of the enzyme surrounded by the α helices, forming a barrel-like structure.[10] Partial barrel, also known as ¾ barrel, structures are more common, consisting of only six alternating α helices and β strands.[13] Partial barrels are more open, or "splayed" and the openness of these partial barrels exposes one face of the β strands, creating a space for the enzyme's active site.

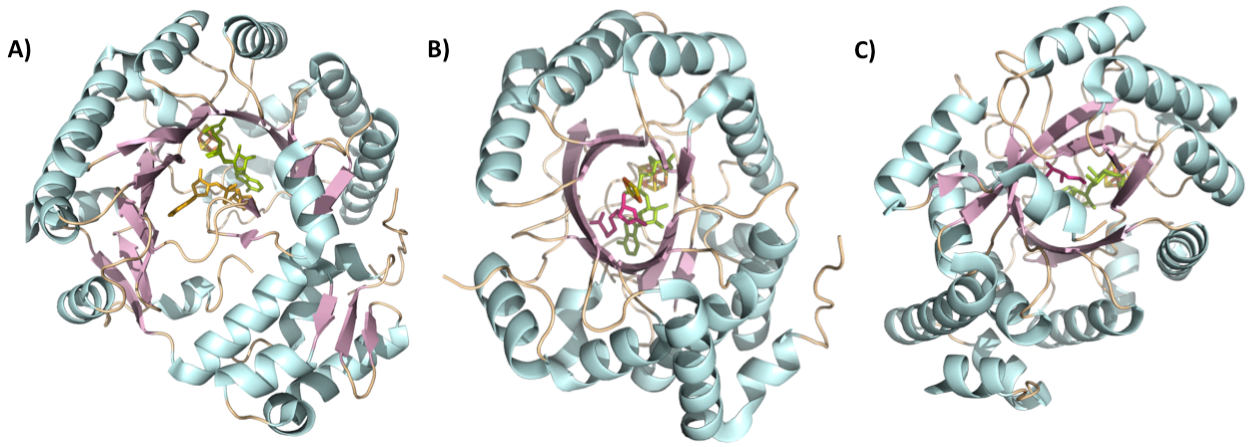

Figure 1.3. Crystal structures of known radical SAM enzymes. **A)** HemN, where [4Fe-4S] cluster is depicted in red and yellow, the cluster-binding SAM molecule in green sticks, and an additional SAM molecule depicted in orange sticks. (PDB ID 1OLT). **B)** BioB, where [4Fe-4S] and [2Fe-4S] clusters are depicted in red and yellow, SAM in green sticks, and ligand $C_{10}H_{18}N_2O_3$ in pink sticks (PDB ID 1R30). **C)** PylB, where [4Fe-4S] cluster is depicted in red and yellow, SAM in green sticks, and ligand $C_6H_{14}N_2O_2$ in pink sticks (PDB ID 3T7V).

The active site is located near the N-terminus of the enzyme, as the loop connecting the first β strand (β1) to the following α helix contains the crucial CX_3CX_2C binding region for the enzyme's catalytic iron-sulfur cluster.[10,13] Openness of the barrel correlates with substrate size, as enzymes that utilize larger substrates have more open barrel structures.[10] Larger barrel openings allow larger substrates to enter and bind in the active site, while smaller barrel openings allow smaller substrates to bind tightly and shield off the active site from surrounding solvent.[10] Portions of the C-terminal region of the enzyme, as well as SAM also aid in shielding the active site from solvent.[10,13] This shielding is particularly important considering the nature of the reactions these enzymes catalyze, as radicals are

extremely reactive and could cause significant harm to the cell if their chemistry is not contained within the enzymes.

The resting oxidation state of the catalytic iron-sulfur cluster is $[4Fe\text{-}4S]^{2+}$, which gets reduced to its catalytically active $[4Fe\text{-}4S]^{1+}$ state by a single electron donor, such as flavodoxin, *in vivo*.[10] This activated cluster is then able to transfer an electron to the nearby SAM molecule, cleaving SAM into methionine and a proposed 5'-deoxyadenosyl radical (dAdo•) intermediate (*Figure 1.4*).[12,14] This radical intermediate is then able to abstract a hydrogen atom from a substrate molecule in the radical SAM enzyme's active site. 5'-deoxyadenosine (dAdoH) is formed, and a reactive substrate-based radical is created.

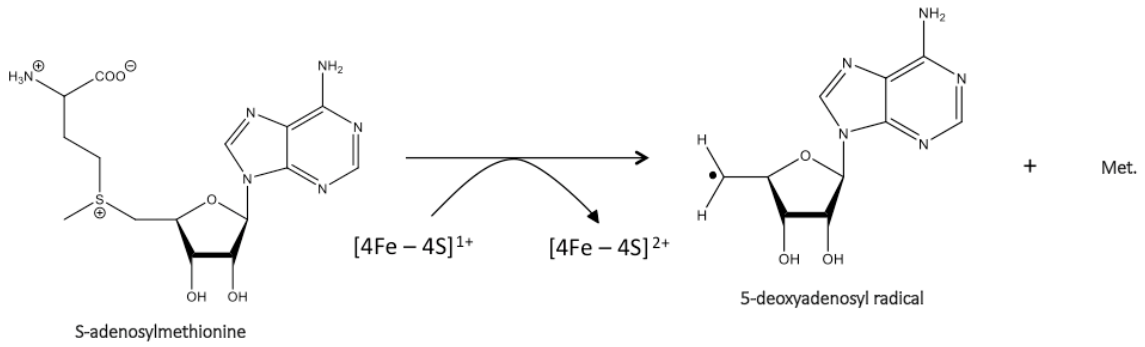

Figure 1.4. General mechanism of action of radical SAM enzymes - SAM cleavage by active $[4Fe\text{-}4S]^{1+}$ cluster and formation of dAdo• intermediate.

Although the highly reactive nature of the dAdo• does not allow for its direct observation, it has been proposed as an intermediate based on stabilized analogs of dAdo• that have been observed with radical SAM enzymes.[10,11] The allylic analog 5'-deoxy-3',4'-anhydroadenosine-5'-yl (anAdo•) was first observed in 1999 by Magnusson, Reed, and Frey, upon replacement of SAM with analog S-3',4'-anhydroadenosyl-L-methionine (anSAM) as a cofactor for the radical SAM enzyme lysine 2,3-aminomutase (LAM) (*Figure 1.5*).[15,16] The same lab also observed the anAdo• intermediate upon reaction of 3',4'-anhydroadenosylcobalamin with the AdoCbl-dependent enzyme diol dehydrase.[17] As AdoCbl enzymes and radical SAM enzymes catalyze analogous reactions, this currently serves as the best evidence for the formation of the dAdo• intermediate in radical SAM reactions.[5]

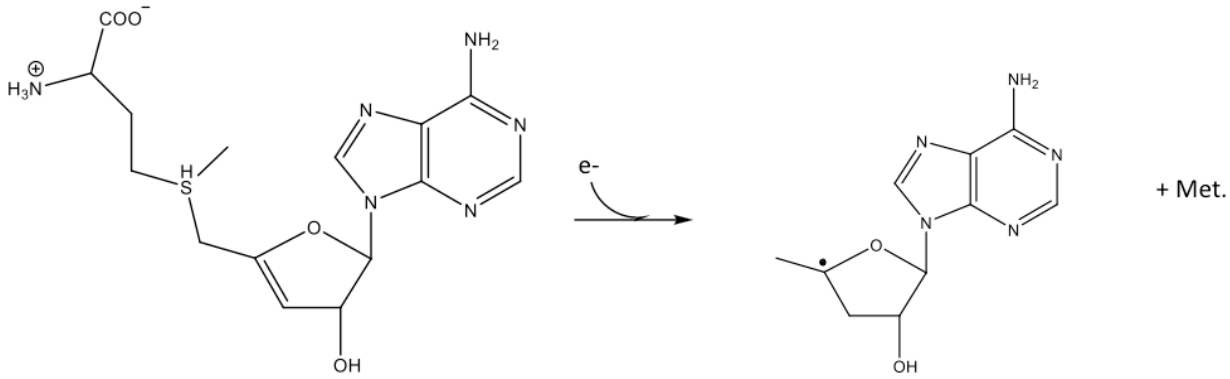

Figure 1.5. Observed cleavage of anSAM into methionine and anAdo• by the radical SAM enzyme LAM.[15,16]

Although the mechanisms of many radical SAM enzymes follow this general scheme, it is important to note that there are many variations within the superfamily. Some radical SAM enzymes also require additional cofactors and clusters for catalysis. For example, BioB also contains a second 2Fe-2S cluster and BtrN utilizes a second 4Fe-4S cluster.[18,19] In other cases, more than one molecule of SAM is required. For example, HemN binds two molecules of SAM, which it likely uses to catalyze two independent carboxylations of its substrate coproporphyrinogen III.[20] One particularly interesting variation in this mechanism is the post-translational modification of bacterial ribosomal RNA (rRNA) by the radical SAM enzyme Cfr (*Figure 1.6*). Cfr is a Class A methyltransferase that affects 23S rRNA of bacteria at the C8 position of adenosine 2503.[10,21,22] The resulting methylated adenosine is located in an antibiotic binding site, and its methylation prevents several classes of antibiotics from binding, thus conferring resistance to many antibiotics that target the large subunit of the ribosome. Some of these antibiotics, like the drug linezolid, are frequently used as the last line of defense against multidrug resistant bacteria, and Cfr has also been linked to methicillin-resistant Staphylococcus aureus (MRSA).[21,22] Understanding the mechanism of Cfr and similar enzymes is therefore a crucial first step in developing effective treatments for such serious bacterial infections.

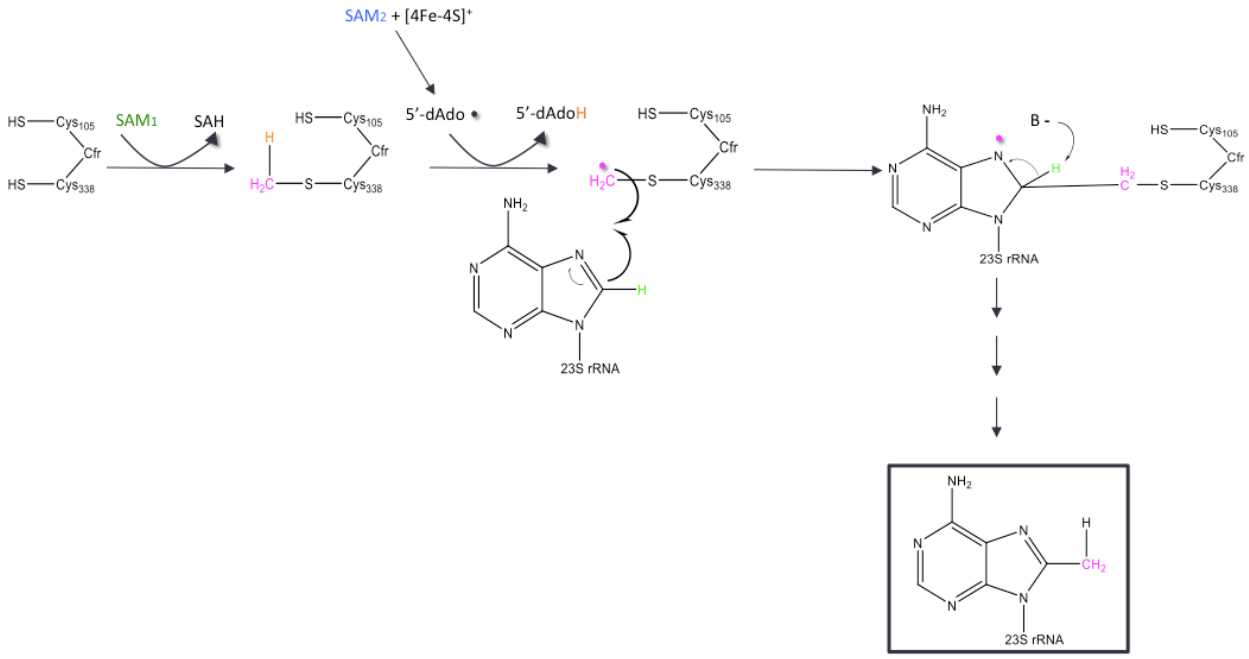

Figure 1.6. Proposed mechanism of methylation by Cfr of C8 on adenosine 2503 in 23S rRNA of the large ribosomal subunit.

In order to catalyze this methylation, Cfr requires two molecules of SAM. A number of mechanisms have been proposed over the years, including a methylene transfer, followed by a hydride shift proposed by Yan & Fujimori in 2011.[23] However, the majority of research supports a mechanism in which the first SAM molecule (denoted in green) utilized by Cfr is cleaved via an S_N2 reaction, forming S-adenosyl-L-homocysteine (SAH) and adding a methyl group to Cys338 of Cfr (*Figure 1.6*).[21,24,25,26] The second molecule of SAM (denoted in blue in *Figure 1.6*) is reductively cleaved into methionine and dAdo• as depicted in Figure 1.1, which then goes on to create a substrate-based radical (denoted in magenta) on A2503 of 23S rRNA (*Figure 1.6*).[21]

Many more suspected members of the radical SAM superfamily also exist, and a number of genes have been identified which contain the CX_3CX_2C motif and other amino acid sequences characteristic to radical SAM enzymes. However, the majority of these suspected members of the radical SAM superfamily remain poorly understood. To date, only 14 enzymes out of the suspected 50,000 have been fully characterized, including a crystal structure.[10] In order to gain a more complete understanding of the superfamily and

their biological significance, it is therefore essential that more of these suspected enzymes are characterized.

For this project, two of these uncharacterized genes were chosen from the structure-function linkage database (SFLD) for further study. The SFLD is a database that classifies sequences of uncharacterized enzymes according to their similarity to known and characterized enzymes.[18] The first enzyme selected from this database, referred to as yfgB, showed sequence similarity to the Class A radical SAM methyltransferases.[18] YfgB was chosen based on the presence of a homolog in the BL21(DE3) *E. Coli* genomic DNA available to the laboratory. The second gene selected, referred to as RS11, codes for an uncharacterized radical SAM enzyme in subgroup 11 (from *Thermotoga neapolitana* DSM 4359, NCBI taxonomy ID: 309803).[18] This subgroup is pyridoxal phosphate (PLP)-dependent, and members show sequence homology to aminomutases.[18,27]

2. MATERIALS & METHODS

2.1 Competent Cell Preparation: Competent DH5-α *E. Coli*, purchased from New England BioLabs (NEB), were prepared for transformations using rubidium chloride. Initially, 5μL of LB media was inoculated with 50μL of NEB5-α and grown overnight at 37°C with 250 rpm shaking. 1mL of this overnight culture was added to 100mL LB media and incubated for an additional 2.75 hours, until OD_{600} reached ~0.7.

The cell growth was then moved to a 4°C cold room and aliquoted into 10mL portions. These portions were incubated on ice for 20 minutes before being centrifuged for 5 minutes at 4°C. Supernatant was discarded and each pellet was re-suspended in 3mL of Buffer TFBI, pH 5.8 [30mM KoAc, 50mM $MnCl_2$, 100mM RbCl, 10mM CaCl2, 15% (v/v) glycerol]. Cells were incubated on ice for 20 minutes with gentle shaking, and centrifuged for an additional 5 minutes at 4°C. Supernatant were again discarded and each pellet was subsequently re-suspended in 400μL of Buffer TFBII, pH 7.0 [10mM NaMOPS, 75mM $CaCl_2$, 10mM RbCl, 15% (v/v) glycerol]. After 30 minutes of incubation on ice, cells were aliquoted into 200μL portions, quickly frozen with liquid nitrogen, and stored long-term at -80°C.

Two 50µL aliquots were also taken for test transformation. Cells were test transformed with a pUC19 plasmid to assess competency. 3µL pUC19 was added to one 50µL portion, while the other 50µL served as a negative control. Both aliquots were heat shocked at 42°C for 30 seconds, then incubated on ice for 5 minutes. 50µL LB growth media was added to each portion, and incubated at 37°C with 250 rpm shaking for 45 minutes. Cells from each aliquot were plated on LB/agar plates containing 50µg/mL ampicillin, and grown overnight at 37°C.

2.2 Amplification & Sequential Digest of yfgB: YfgB (1155 b.p.) was amplified from BL21(DE3) *E. Coli* genomic DNA by polymerase chain reaction (PCR). Reaction volumes were 50 µL total, and each reaction tube contained the following: 32.5µL sterile H_2O, 5µL 10X Sigma-Aldrich PCR buffer, 3µL MgCl2, 3µL forward primer (sequence: 5' CATAGGATCCATGTCTGAACAATTAGTCAC 3'), 3µL reverse primer (sequence: 5' TATAGCTAAGCTCAGACCGCTTTAATGTC 3'), 2µL 100X plasmid DNA, 1µL dNTP's, 0.5µL Taq polymerase. Reactions were run using the following parameters - Step 1: 1x denaturing at 95°C for 3 minutes; Step 2: 34x denaturing at 95°C for 30 seconds, annealing at 52°C, and extension at 72°C for 1 minute, 15 seconds; Step 3: 1x extension at 72°C for 5 minutes, and stored at -20°C.

Agarose gel electrophoresis was used to confirm amplification of yfgB, which was subsequently extracted from the gel using a Sigma-Aldrich GenElute Gel Extraction Kit. YfgB was then digested with the restriction enzyme Blp1 by incubating 20µL amplified yfgB, 5µL NEB CutSmart buffer, 1µL Blp1, and 24µL sterile H_2O at 37°C for 1 hour. Following the digest, yfgB was again detected using agarose gel electrophoresis and extracted using a Sigma-Aldrich GenElute Gel Extraction Kit. A second digest with the restriction enzyme BamH1 was performed by incubating 25 µL of that DNA, 5 µL NEB buffer 3.1, 0.5µL BamH1, and 19.5µL sterile H_2O at 37°C for 1 hour. The results of this digest were also visualized using agarose gel electrophoresis, and digested DNA was again extracted from the gel.

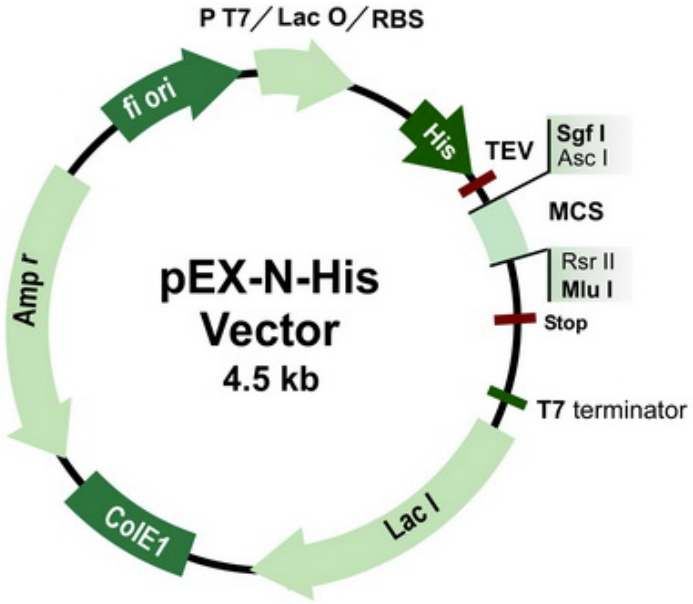

Figure 2.3.1. Bacterial expression vector pEX-N-His purchased from Blue Heron Gene Company containing the RS11 plasmid. OriGene product manual, Catalog No. PS100030).

2.3 Transformation of RS11 into BL21 (DE3): A pEX-N-His bacterial expression vector was purchased from Blue Heron Gene Company already containing the RS11 plasmid and an N-terminal 6X Histidine tag (*Figure 2.3.1*). 5µL of 5ng/µL purified RS11 plasmid DNA was transformed into 0.5mL BL21(DE3) competent *E. Coli* obtained from New England BioLabs. Following transformation, 1:10, 1:100, and 1:1000 dilutions of transformed cells were plated on LB/agar plates containing 50µg/mL ampicillin, and grown overnight at 37°C.

2.4 BL21(DE3) Growth & Overexpression of RS11: RS11 colonies were grown from transformed BL21(DE3) *E. Coli* cells. At the time of overexpression, one colony was used to inoculate 5mL LB media containing 50µg/mL ampicillin, and grown overnight at 37°C with 250 rpm shaking. Multiple 5mL overnight growths were performed simultaneously.

5 – 15 mL of overnight culture was added to 1 L of LB media, which contained ampicillin at a concentration of 50µg/mL. The mixture was incubated at 37°C with 250 rpm shaking. Starting at 3 hours of incubation time, OD_{600} was monitored in 10 – 15 minute intervals. Upon reaching OD_{600} of 0.5 – 0.6, isopropyl β-D-1-thiogalactopyranoside (IPTG) was added to a final concentration of 1 mM in order induce protein expression, and incubation at 37°C with 250 rpm shaking was continued for an additional 3 hours. Cells were then harvested using centrifugation for 10 minutes at 6,000 rpm and 4°C. Pellets were quickly frozen with liquid nitrogen and stored long-term at -80°C. Separate pellets were also obtained prior to, and following induction with IPTG, in order to confirm protein overexpression.

2.5 Purification of RS11: Cell pellets were thawed at 4°C and re-suspended in ~2 mL lysis buffer per gram of pellet. Lysis buffer consisted of 200 mM NaCl, 10 mM sodium phosphates, 10 mM imidazole, 5% (w/v) glycerol, 1 mM phenylmethylsulfonyl fluoride (PMSF; dissolved in methanol), lysozyme (final conc. 8mg/50mL), 10 mM MgCl2, 1% (v/v) Triton X-100, and ~5µg/mL of both RNase A and DNase I. The mixture was homogenized with a syringe and an 18-gauge needle every 5-10 minutes, for a total of 45 minutes, at 4°C. Then, the homogenate was centrifuged for 30 minutes at 18,000 rpm and 4°C.

The supernatant (cell lysate) from this centrifugation was then loaded on to an affinity column containing nickel nitrilotriacetic acid (NTA) resin purchased from Sigma-Aldrich, which had been regenerated following previous uses. Just before purification, the resin was equilibrated with 10 column volumes (CV's) Buffer A [200mM NaCl, 20mM sodium phosphates – pH 7.4, 10mM imidazole, 5% (w/v) glycerol]. After the cell lysate was loaded onto the column, the resin was again washed with 10 CV's Buffer A. Then, a gradient of Buffer B [200mM NaCl, 20mM sodium phosphates – pH 7.4, 500mM imidazole, 5% (w/v) glycerol] was used to elute the protein as follows – 5 CV's 10% Buffer B (diluted with Buffer A), 5 CV's 20% Buffer B, 5 CV's 50% Buffer B, 10 CV's 100% Buffer B. 0.5mL fractions were taken during the first three steps of the elution gradient, while 1mL fractions were taken during the final step of the gradient. 50µL aliquots were also taken of every third fraction from the gradient, as well as of the cell lysate flow-through and wash flow-through, for analysis with SDS-PAGE.[28]

3. RESULTS & DISCUSSION

3.1 Competent Cell Preparation: Following test transformation with vector pUC19, colonies were counted, and NEB DH5α *E. Coli* prepared with rubidium chloride showed greatly increased competence compared to previous cells made in the lab using calcium chloride.

***3.2 Amplification & Sequential Digest of yfgB*:** An initial attempt at PCR amplification of yfgB (1155 b.p.) was made in two separate reaction tubes using genomic DNA that was previously extracted from BL21(DE3) *E. Coli*. This first PCR attempt of yfgB was successful

in both reaction tubes, however the first reaction tube (tube 1.0) showed significantly less amplification than the second reaction tube (tube 2.0). The results of the first digest with restriction enzyme Blp1 were inconclusive, as there is no visible difference in migration between digested and undigested samples of yfgB when detecting using agarose gel electrophoresis (*Figure 3.1.1a*). Successful digestion with Blp1 can only be confirmed when yfgB is ligated into pET14b, however, the gel did show that there was a sufficient concentration of Blp1 digested yfgB to continue with. In case the first digest was in fact successful, the second restriction enzyme digest with BamH1 was attempted. Following this digest, no DNA whatsoever was seen on an agarose gel, indicating that the DNA samples digested were not sufficiently concentrated (*Figure 3.1.1b*). Another attempt was made using increased amounts of DNA (2.5X the original concentration) to digest the remaining samples with BamH1, however agarose gel electrophoresis again showed no sign of DNA.

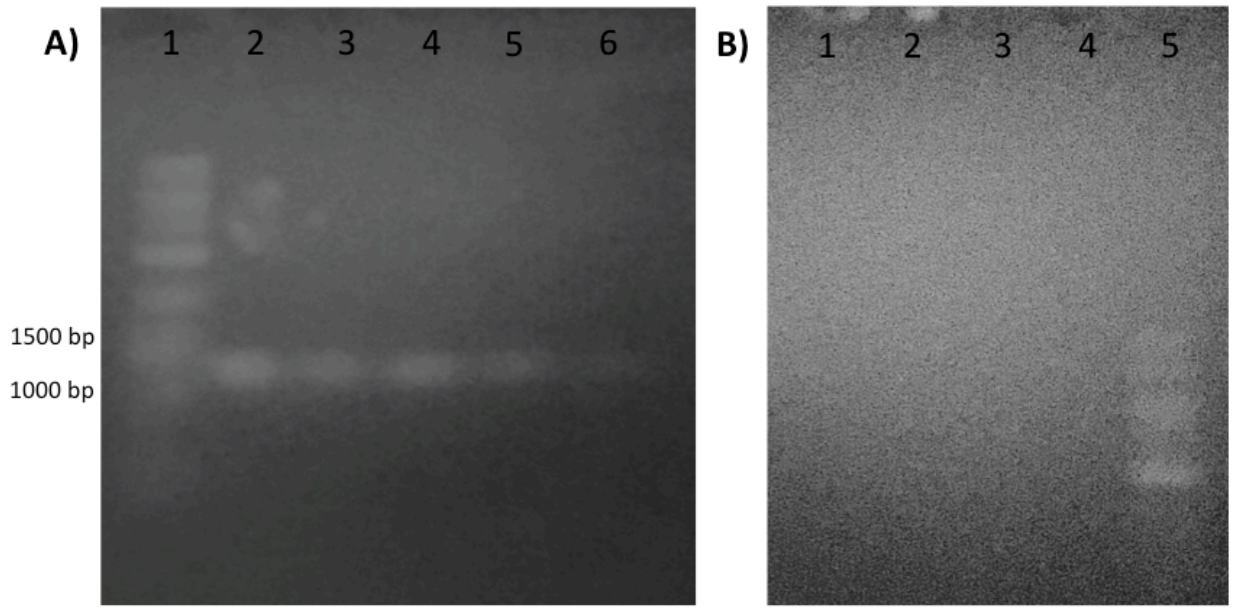

Figure 3.1.1. Sequential restriction enzyme digests of amplified yfgB. Agarose gel electrophoresis, stained in 0.3µg/mL EtBr. **A)** Amplified yfgB digested with Blp1. Lane 1: NEB 1kb DNA ladder; lane 2: undigested yfgB, PCR reaction tube 1.0; lane 3: yfgB digested with Blp1, PCR reaction tube 1.0; lane 4: undigested yfgB, PCR reaction tube 2.0; lanes 5-6: yfgB digested with Blp1, PCR reaction tube 2.0. **B)** Amplified yfgB digested with Blp1, then with BamH1. Lanes 1-2: yfgB digested with Blp1 and BamH1, PCR reaction tube 2.0; lanes 3-4 PCR yfgB digested with Blp1 and BamH1, PCR reaction tube 1.0; lane 5: NEB 1kb DNA ladder.

At this point, it was decided that in order to get a sufficient concentration of DNA following the second restriction enzyme digest, the amount of amplified yfgB used for the first restriction enzyme digest needed to be increased. The same PCR method was used as before to generate enough amplified DNA, however this time neither of the two reaction tubes showed evidence of successful yfgB amplification (*Figure 3.1.2a*). Since this method had been successfully used before, it is not known exactly why there was no amplification. Based on the variability in the amount of amplification achieved previously, it seemed possible that the PCR method needed further optimization to get consistent results. The first alteration made was an increase in the amount of primers used for the reaction. The volume of both forward and reverse primers used was doubled from the original method, as increased primer concentration has been found to increase the amount of amplified product in later cycles of PCR.[29] Two reaction tubes were run using this altered method, however neither showed evidence of successful yfgB amplification (*Figure 3.1.2b*).

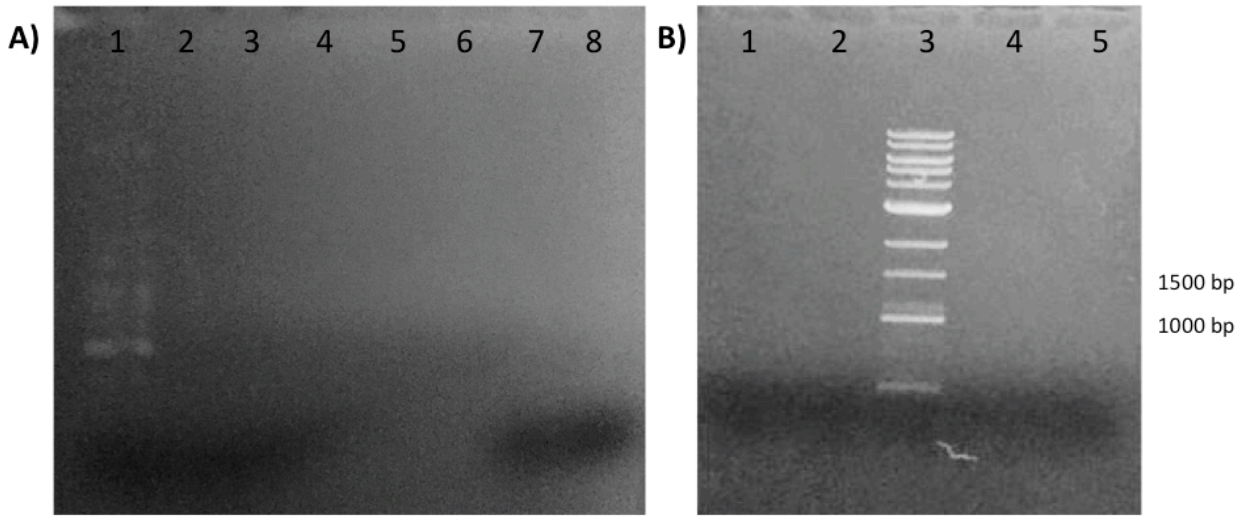

Figure 3.1.2. Additional attempts to amplify yfgB using PCR. Agarose gel electrophoresis, stained in 0.3µg/mL EtBr. **A)** Lane 1: NEB 1kb DNA ladder; lanes 2-3 yfgB, PCR reaction tube 1.1; lanes 4-6: empty; lanes 7-8: yfgB, PCR reaction tube 2.1. **B)** Lanes 1-2: yfgB, PCR reaction tube 1.2; lane 3: NEB 1kb DNA ladder; lanes 4-5: yfgB PCR reaction tube 2.2.

Following this additional failure to amplify yfgB, a number of additional factors were considered for the cause. One potential issue was the dNTP samples being used. DNTP's are particularly susceptible to degradation by DNase, and aliquots may have been contaminated throughout repeated uses. In future reactions, care was taken to use fresh,

full vials of dNTP's each time. Additionally, the enzyme Taq polymerase used to catalyze the incorporation of these dNTP's into the DNA was nearing the end of a sample shared with multiple other students. It is possible that over time, the Taq was slowly denatured and lost its effectiveness.

Once new Taq was purchased, the previous method was re-attempted using these new materials. For unknown reasons, the EtBr migrated an unusually large amount towards the negative electrode and nothing was visible, including the ladder. The gel was saved overnight in 1X TAE buffer and post-stained the following day in EtBr, however at this point any bands that may have been present had diffused. The exact PCR procedure was then repeated in two reaction tubes, and the agarose gel stained in additional EtBr immediately following electrophoresis. From the first reaction tube, bands of yfgB DNA were visible near 1000 b.p. on the agarose gel. As yfgB is ~1155 b.p. in length, these bands are consistent with amplification of yfgB (*Figure 3.1.3a*). The agarose gel showed no signs of yfgB amplification in the second reaction tube. Considering both reaction tubes were run using the same materials, it is unknown why the second tube showed no evidence of amplification. In order to increase the concentration of yfgB available for the first restriction enzyme digest, the remaining sample from the first reaction tube was run on an agarose gel and all bands of amplified yfgB were extracted (*Figure 3.1.3b*).

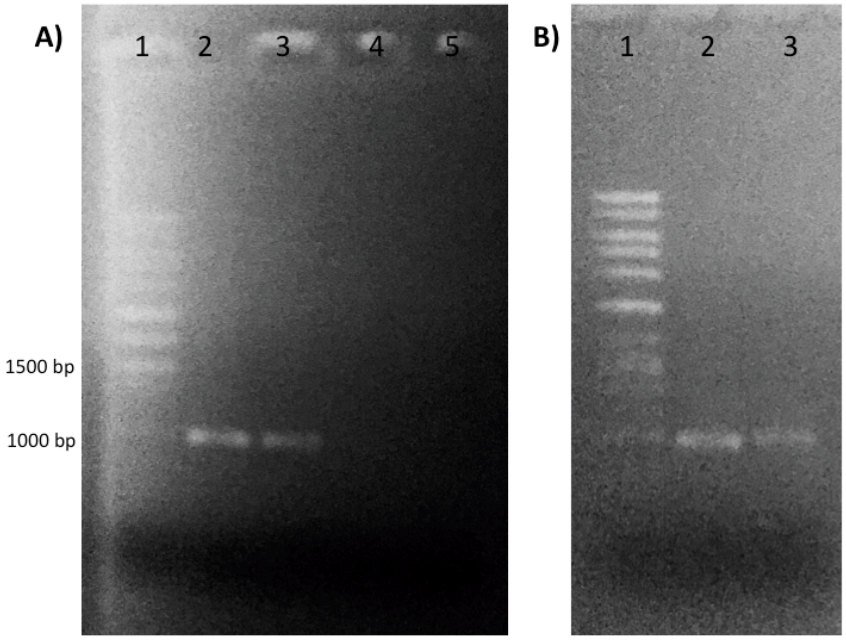

This sample was then digested with the restriction enzyme Blp1, however the volume of DNA used for the digestion was doubled from previous attempts to 20μL. Agarose gel electrophoresis confirmed that the digest was in fact successful (*Figure 3.1.4a*). Following extraction from the agarose gel, the DNA was then digested with the restriction enzyme BamH1. The volume of yfgB used for the digest was doubled to 50μL from the previous attempt at BamH1 digestion. As there is no visible change in location of the yfgB bands on an agarose gel from Blp1 digestion to BamH1 digestion, the success of the BamH1 digestion cannot be confirmed until the DNA is ligated into a bacterial expression vector. However, this time there was a sufficient concentration of DNA following digestion with BamH1 to have visible bands on an agarose gel, and these bands were extracted in order for use in ligation.

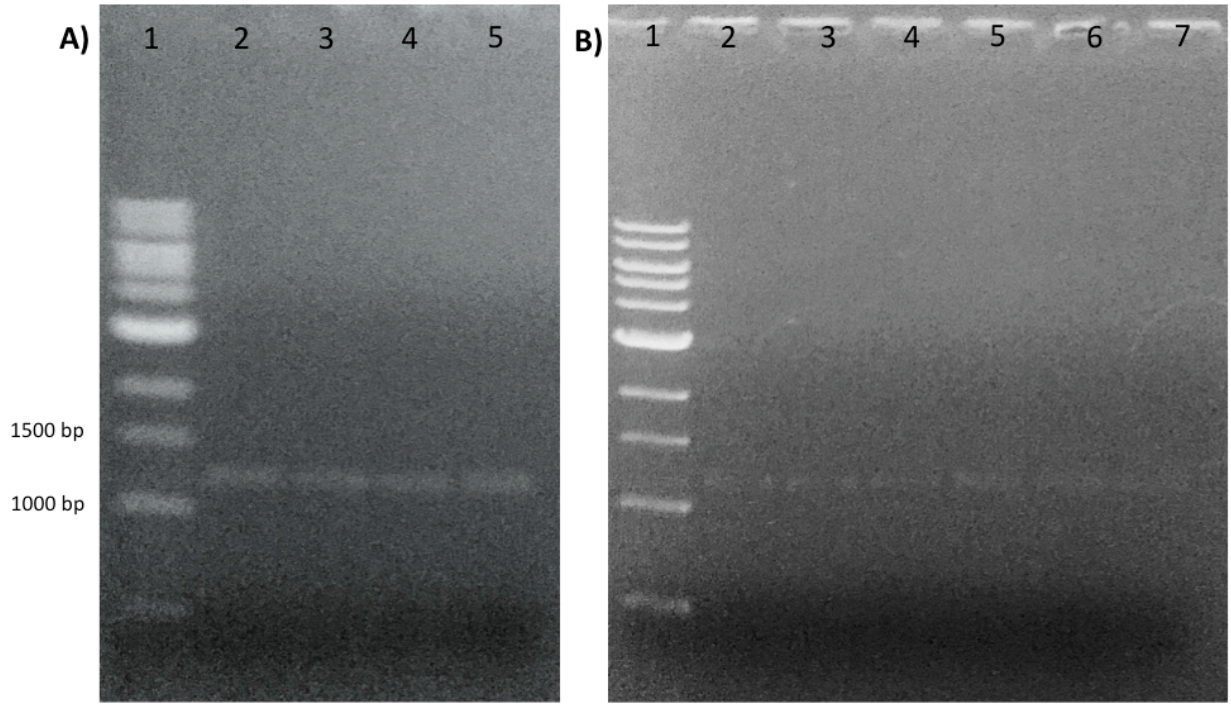

Figure 3.1.4. Agarose gel electrophoresis, stained in 0.3µg/mL EtBr. **A)** Digestion of amplified yfgB with Blp1. Lane 1: NEB 1kb DNA ladder; lanes 2-5: yfgB digested with Blp1, PCR reaction tube 1.3. **B)** Digestion of amplified yfgB with Blp1 and BamH1. Lane 1: NEB 1kb DNA ladder; lanes 2-5: yfgB digested with Blp1 and BamH1, PCR reaction tube 1.3.

3.3 BL21(DE3) Growth & Overexpression of RS11: In the initial attempt, difficulty was met in growing enough cells for protein expression. Methods previously developed in the lab called for one 5mL "starter tube" of BL21(DE3) overnight culture per 1L of media used the day of growth. However, when 1L of LB media was inoculated with 5mL of overnight culture, there was insufficient growth of BL21(DE3) in the media. OD_{600} of the growth media must reach ~0.6 before IPTG induction in order to ensure that enough cells are present for optimal protein expression. However, after being incubated for >5 hours, the media was still at an OD_{600} of ~0.25. Due to time limitations, IPTG induction was still attempted, with the expectation that cell yields would be decreased. As suspected, cell yield for that batch was only 0.658g/L.

In the next batch of growth, the amount of overnight culture used was doubled to 10mL per 1L of LB media. After 4 hours of inoculation OD_{600} was still only ~0.4, so an additional 5mL of overnight culture was added to the media at this time. Only an additional

0.5 hour was needed for the OD_{600} of that batch to reach ~0.6. Inducing at this higher OD_{600} increased cell yield to 1.673g/L, a significant increase in yield compared to the previous attempt.

Based on time restrictions, the goal was to reach OD_{600} of ~0.6 within 3 hours, in order to allow sufficient time for maximal protein expression to occur after induction with IPTG. In the following growth, 1L of media was therefore inoculated with 15mL overnight culture to begin with. Time to OD_{600} of ~0.6 was ~3.25 hours, and a cell yield of 1.120g/L was obtained. Although cell yield appeared to decrease slightly using this method, it was continued in future growths in order to fit time limitations. Once the method was optimized, pellets were obtained pre- and post-induction with IPTG to check for protein expression. The SDS-PAGE gel appeared overloaded and so any difference in RS11 protein levels (MW 32.6kD) before and after IPTG induction was not visible. No sample remained that could have been used to run an additional gel.

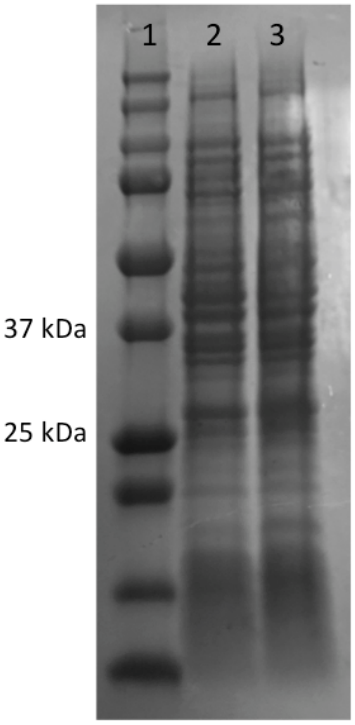

Figure 3.3.1. SDS-PAGE electrophoresis stained in AcquaStain protein gel stain. Lane 1: BioRad Dual Color Precision Plus prestained protein standard; lane 2: pellet obtained from cell growth pre-induction with IPTG; lane 3: pellet obtained from cells 3 hours post-induction with IPTG.

Three additional batches of cell growth and protein expression were performed using the optimized method. Average cell yield for those batches was 2.06g/L. Unfortunately, SDS-PAGE analysis of pre- and post-IPTG induction pellets from those batches showed no sign of increased protein expression following induction of the cells with IPTG (*Figure 3.3.2*).

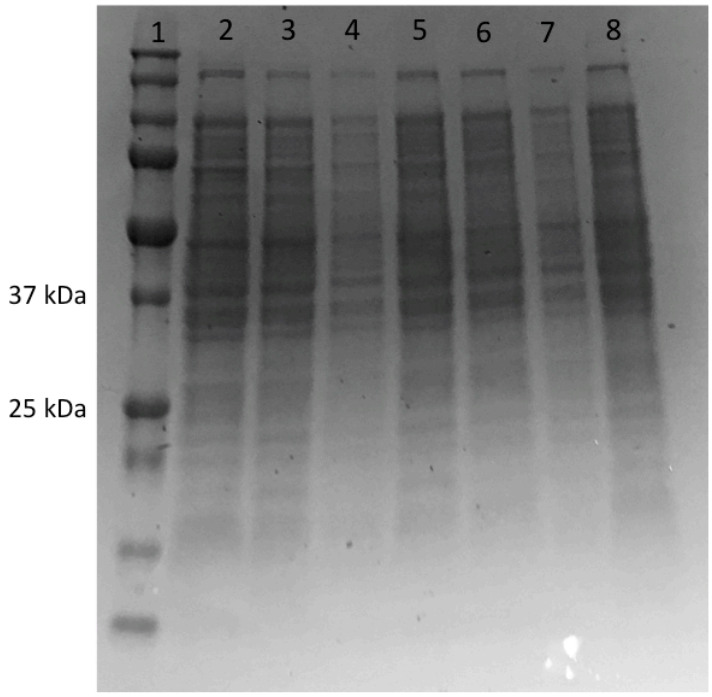

Figure 3.3.2. SDS-PAGE electrophoresis stained in AcquaStain protein gel stain. Lane 1: BioRad Dual Color Precision Plus prestained protein standard; lanes 2-3: pellets obtained pre- and 3 hours post-IPTG induction, respectively, from cell growth 1.4; lane 4: pellet obtained pre-IPTG induction from cell growth 1.5 – perforated well; lanes 5-6: pellets obtained pre- and 3 hours post-IPTG induction, respectively, from cell growth 1.5; lanes 7-8: pellets obtained pre- and 3 hours post-IPTG induction, respectively, from cell growth 1.6.

3.4 Purification of RS11:

In case protein expression had been successful in small amounts that were not visible on the PAGE gel, the samples from the first three batches of growth and expression were combined and purified. SDS-PAGE electrophoresis of fractions collected during purification revealed a number of problems. First, the regenerated nickel resin being used was not binding the 6X Histidine tag properly and all of the cell contents, including any RS11 protein, flowed through the column immediately with the cell lysate. Additionally,

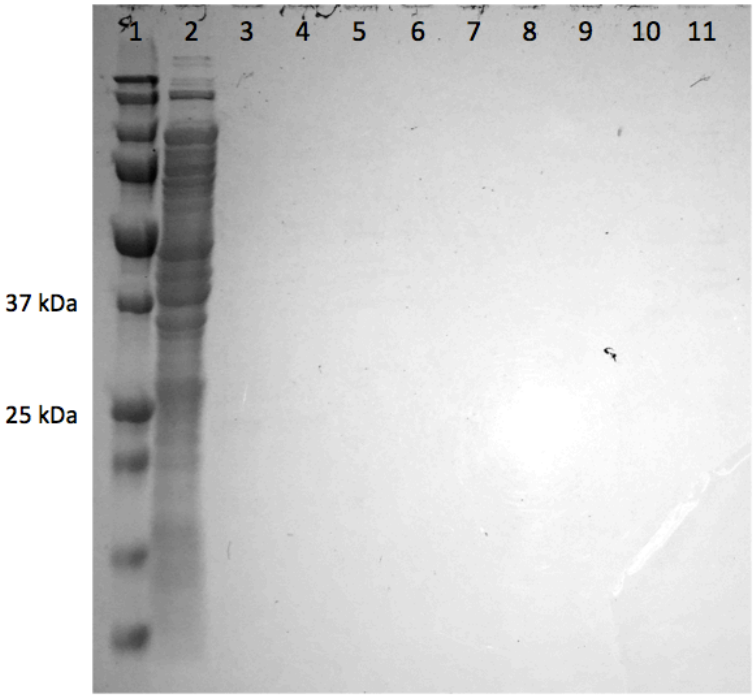

Figure 3.4.1. SDS-PAGE electrophoresis stained in AcquaStain protein gel stain. Lane 1: BioRad Dual Color Precision Plus prestained protein standard; lane 2: cell lysate flow-through from nickel-affinity column; lanes 3-11: every third fraction collected during protein elution on a nickel-affinity column.

analysis of the cell lysate on an SDS-PAGE gel revealed an overall lack of protein expression (*Figure 3.4.1*).

3.5 Transformation of RS11 into BL21(DE3): Due to lack of success in protein expression using glycerol stock solutions of BL21(DE3) *E. Coli* containing the RS11 plasmid, purified plasmid was transformed into fresh BL21(DE3) cells. Out of the three dilutions of transformed cells that were plated, only the first 1:10 dilution grew any colonies. These will be used for future attempts at expressing RS11 in BL21(DE3) *E. Coli*.

4. CONCLUSION & FUTURE DIRECTIONS

At this time, no significant strides in elucidating the mechanism of the enzyme coded for by yfgB, or in identifying its substrates. However, progress was made in obtaining a concentrated sample of sequentially digested yfgB. Digestion of the bacterial expression vector pET14b is underway, and it is expected that few difficulties will be encountered in ligating yfgB into pET14b. Additionally, competent DH5α *E. Coli* prepared using rubidium chloride showed significantly greater competence than previous competent cells used in the lab, and it is predicted that yfgB can be successfully transformed into these cells. In order to confirm successful insertion of the yfgB gene into the DH5α *E. Coli*, gene sequencing will be used. Once this is completed, growth, expression, and purification of yfgB will be attempted using the method described in sections 2.4-2.5.

Additionally, at this time RS11 is unable to be confirmed as a radical SAM enzyme. Difficulties were encountered at numerous steps during cell growth and protein expression that prevented a purified sample of the RS11 enzyme from ever being obtained for analysis. Before any mechanistic investigations can be done, progress must be made in inducing the BL21(DE3) *E. Coli* with IPTG to express RS11. As fresh BL21(DE3) *E. Coli* have recently been transformed with the RS11 plasmid, there is potential for successful cell growth and protein expression in the near future using these new cells. Additionally, new nickel NTA resin has been purchased, as the regenerated resin used no longer had sufficient binding capacity for purification.

Once purified samples of overexpressed yfgB and/or RS11 are obtained, confirmation of these proteins as radical SAM enzymes and analysis of their activity can begin. Electron paramagnetic resonance (EPR) will be used to confirm the presence of a reducible [4Fe-4S] cluster; the $[4Fe\text{-}4S]^{2+}$ form of the cluster is EPR silent, but upon reduction to the catalytically active $[4Fe\text{-}4S]^{1+}$ the cluster becomes EPR active.[30] SAM cleavage assays can also be performed and monitored via HPLC for the production of dAdoH and methionine.[30]

REFERENCES

1. Sofia, H.J., Chen, G., Hetzler, B.G., Reyes-Spindola, J.F., Miller, N.E.; Radical SAM, a novel protein superfamily linking unresolved steps in familiar biosynthetic pathways with radical mechanisms: functional characterization using new analysis and information visualization methods. *Nucleic Acids Res.* **2001**. *29*, 1097-1106.

2. Guianvarc'h, D., Florentin, D., Tse Sum Bui, B., Nunzi, F., Marquet, A.; Biotin synthase, a new member of the family of enzymes which uses S-adenosylmethionine as a source of deoxyadenosyl radical. *Biochem Biophys Res Commun* **1997**, *236(2),* 402-406.

3. Mahanta, N., Fedoseyenko, D., Dairi, T., Begley, T.P.; Menaquinone biosynthesis: formation of aminofutalosine requires a unique radical SAM enzyme. *J Am Chem Soc* **2013**, *135(41),* 15318-15321.

4. Layer, G., Verfürth, K., Mahlitz, E., Jahn, D. Oxygen-independent coproporphyrinogen-III oxidase HemN from Escherichia coli. *J Biol Chem* **2002**, *277(37),* 34136-34142.

5. Benjdia, A., Leprince, J., Guillot, A., Vaudry, H., Rabot, S., Berteau, O.; Anaerobic sulfatase-maturing enzymes: radical SAM enzymes able to catalyze in vitro sulfatase post-translational modification. *J Am Chem Soc* **2007**, *129(12),* 3462-3463.

6. Fang, Q., Peng, J., Dierks, T.; Post-translational formylglycine modification of bacterial sulfatases by the radical S-adenosylmethionine protein AtsB. *J Biol Chem* **2004**, *279(15),* 14570-14578.

7. Rebeil, R., Nicholson, W.L.; The subunit structure and catalytic mechanism of the Bacillus subtilis DNA repair enzyme spore photoproduct lyase. *Proc Natl Acad Sci U S A*, **2001**, *98(16),* 9038-9043.

8. Kehrenberg, C., Schwarz, S., Jacobsen, L., Hansen, L.H., Vester, B.; A new mechanism for chloramphenicol, florfenicol, and clindamycin resistance: methylation of 23S ribosomal RNA at A2503. *Mol Microbiol* **2005**, *57(4),* 1064-1073.

9. Long, K.S., Poehlsgaard, J., Kehrenberg, C., Schwarz, S., Vester, B.; The Cfr rRNA methyltransferase confers resistance to Phenicols, Lincosamides, Oxazolidinones, Pleuromutilins, and Streptogram A antibiotics. *Antimicro Agents Chemother* **2006**, *50(7),* 2500-2505.

10. Broderick J.B., Duffus B.R., Duschene K.S., Shepard E.M.; Radical S-adenosylmethionine enzymes. *Chem Rev* **2014**, *114*, 4229-4317.

11. Layer G., Heinz D.W., Jahn D., Schuber W.D.; Structure and function of radical SAM enzymes. *Curr Opin Chem Biol* **2004**. *8*, 468-476.

12. Walsby, C.J., Ortillo, D., Broderick, W.B., Broderick, J.B., Hoffman, B.M.; An anchoring role for FeS clusters: chelation of the amino acid moiety of S-adenosylmethionine to the unique iron site of the [4Fe-4S] cluster of pyruvate formate-lyase activating enzyme. *J Am Chem Soc* **2002**, *124(38),* 11270-11271.

13. Vey J.L., Drennan, C.L.; Structural insights into radical generation by the radical SAM superfamily. *Chem Rev* **2011**, *111*, 2487-2506.

14. Walsby, C.J., Hong, W., Broderick, W.B., Cheek, J., Ortillo, D., Broderick, J.B., Hoffman, B.M.; Electron-nuclear double resonance spectroscopic evidence that S-adenosylmethionine binds in contact with the catalytically active [4Fe-4S]+ cluster of pyruvate formate-lyase activating enzyme. *J Am Chem Soc* **2002**, 124(12), 3143-3151.

15. Magnusson, O.T., Reed, G.H., Frey, P.A.; Spectroscopic evidence for the participation of an allylic analogue of the 5'-deoxyadenosyl radical in the reaction of lysine 2,3 aminomutase. *J Am Chem* Soc **1999**, *121*, 9764-9765.

16. Magusson, O.T., Reed, G.H., Frey, P.A.; Characterization of an allylic analogue of the 5'-deoxyadenosyl radical: an intermediate in the reaction of lysine 2,3-aminomutase. *Biochemistry*, **2001**, *40*, 7773-7782.

17. Mansoorabadi, S.O., Magnusson, O.T., Poyner, R.R., Frey, P.A., Reed G.H.; Analysis of the cob(II)alamin – 5'-deoxy-3',4'-anhydroadenosyl radical triplet spin system in the active site of diol dehydrase. *Biochemistry* **2006**, *45(48),* 14362-14370.

18. Akiva, E., Brown, S., Almonacid, D.E., Barber A.E., Custer, A.F, Hicks, M.A., Huang, C.C., Lauck, F., Mashiyama, S.T., Meng, E.C., Mischel, D., Morris, J.H., Ojha, S., Schnoes, A.M., Stryke, D., Yunes, J.M., Ferrin, T.E., Holliday, G.L., Babbitt, P.C.; The structure-function linkage database. *Nucl Acids Res* **2014**, *42*, D521-D530.

19. Grove, T.L., Ahlum, J.H., Sharma, P., Krebs, C., Booker, S.J.; A consensus mechanism for radical SAM-dependent dehydrogenation? BtrN contains two [4Fe-4S] clusters. *Biochemistry* **2010**, *49(18),* 3783-3785.

20. Layer, G., Grage, K., Teschner, T., Shünemann, V., Breckau, D., Masoumi, A., Jahn, M., Heathcote, P., Trauwein, A.X., Jahn, D.; Radical S-adenoslmethionine enzyme coproporphyrinogen III oxidase HemN: functional features of the [4Fe-4S] cluster and the two bound S-adenosyl-L-methionines. *J Biol Chem* **2005**, *280(32),* 29038-29046.

21. Yan, F., LaMarre, J.M., Rörich, R., Wiesner, J., Jomaa, H., Mankin, A.S., Fjuimori, D.G.; RlmN and Cfr are radical SAM enzymes involved in methylation of ribosomal RNA. *J Am Chem Soc* **2010**, *132(11),* 3952-3962.

22. Booth, M.P.S., Challand, M.R., Emery, D.C., Roach, P.L., Spencer, J.; High-level expression and reconstitution of active Cfr, a radical-SAM rRNA methyltransferase that confers resistance to ribosome-acting antibiotics.

23. Yan, F., Fujimori, D.G.; RNA methylation by radical SAM enzymes RlmN and Cfr proceeds via methylene transfer and hydride shift. *PNAS* **2011**, *108(10),* 3930-3934.

24. Boal, A.K., Grove, T.L., McLaughlin, M.I., Yennawar, N.H., Booker, S.J.; Structural basis for methyl transfer by a radical SAM enzyme. *Science*, **2011**, *332(6033),* 1089-1092.

25. Grove, T.L., Benner, J.S., Radle, M.I., Ahlum, J.H., Landgraf, B.J., Krebs, C., Booker, S.J.; A radically different mechanism for S-adenosylmethionine-dependent methyltrasnferases. *Science*, **2011**, *332*, 604-607.

26. Grove, T.L., Radle, M.I., Krebs, C., Booker, S.J.; Cfr and RlmN contain a single [4Fe-4S] cluster, which directs two distinct reactivities for S-adenosylmethionine: methyl transfer by S_N2 displacement and radical generation. *J Am Chem Soc* **2011**, *133(49),* 19586-19589.

27. Frey, P.A., Reed, G.H.; Pyridoxal-5'-phosphate as the catalyst for radical isomerization in the reactions of PLP-dependent aminomutases. *Biochimica et Biophysica Acta 1814*, **2011**, 1548-1557.

28. Hutcheson, R.A.U. Mechanistic and Spectroscopic Investigations of Pyruvate Formate-Lyase Activating Enzyme. Ph. D. Dissertation, Montana State University, Bozeman, MT, **2012**.

29. Czerny, T.; High primer concentration improved PCR amplification from random pools. *Nucl Acids Res* **1996**, *24(5)*, 985-986.

30. Duschene, K.S., Broderick, J.B.; The antiviral protein viperin is a radical SAM enzyme. *FEBS Letters* **2010,** *584,* 1263-1267.